TRABAJOS DE PREHISTORIA
79, N.º 1, enero-junio 2022, pp. S1-S21, ISSN: 0082-5638
https://doi.org/10.3989/tp.2022.12287

Ceramic production and household organisation of Late Bronze Age communities: forming processes and spatial distribution of the ceramic vessels of Genó (north-eastern Iberian peninsula)*

Producción de cerámicas y organización doméstica en las comunidades del Bronce final: procesos de modelado y distribución espacial de los recipientes cerámicos de Genó (noreste de la península ibérica)

Javier Cámara Manzaneda[a], Jaume García Rosselló, Francisco Javier López-Cachero and Xavier Clop García

Annex: Supplementary File

Anexo: archivo complementario

* The Generalitat de Catalunya funded the research of groups Grup de Recerques Arqueològiques al Mediterrani i al Proper Orient (GRAMPO) (SGR 2017-1302) and Seminari d'Estudis i Recerques Prehistòriques (SERP) (SGR 2017-00011), as well as the predoctoral fellowship FI-DGR-2017 (n.º 00567) to JCM. Ministerio de Economía y Competitividad - MINECO (Spain) funded two projects "Arqueobioquímica de la alimentación durante el Neolítico peninsular. Nuevos marcadores y referenciales para el estudio de las pautas de producción y consumo en arqueología" (HAR2017-88304-P, IPs María Saña and XCG), and "Familias, vecinos y forasteros en la prehistoria reciente del prelitoral catalán" (HAR2017-87695-P, IP FJL-C).
[a] Corresponding author: Javier Cámara Manzaneda. Laboratory ARCHAEOM, Dept. de Prehistòria. Universitat Autònoma de Barcelona. Edifici B. 08193 Bellaterra. Barcelona. Spain. E-mail: javier.camara@uab.es

Copyright: © 2022 CSIC. Este es un artículo de acceso abierto distribuido bajo los términos de la licencia de uso y distribución "Creative Commons Reconocimiento 4.0 Internacional" (CC BY 4.0)

MATERIALS AND METHOD

The ceramic typology of Genó has been extensively developed in successive works[1] (Maya *et al.* 1998). The main characteristics of the seven basic types are the following:

F1. Carinated vessels with an S-shaped profile and curved outward rim. This is the largest group, accounting for 77% of all the ceramic elements recovered from the site. A total of seven sub-types can be distinguished, thanks mainly to the proportionality and size indexes[2].

F2. Non-carinated vessels with an S-shaped profile and curved outward rim. This type presents a wide variety of sizes, with the largest vessels predominating. In this case we have also differentiated between seven different sub-types based on the variations in profile and size since the capacities range from 1 to 90 l. It is the second most-represented group in the ceramic assemblage with a total of 13%.

F3. Non-carinated vessels with a closed structure and inward rim. We have been able to distinguish five sub-types defined by their formal characteristics and size, which is the key factor. This group makes up 6% of the ceramics.

F4. Vessels with an open structure and outward rim. These are characterised by a continuous profile from the base to the rim without any rupture points on the profile, and the maximum diameter corresponds to the diameter of the rim. This group is composed of only four vessels.

F5. Supports. These are made up of two more or less symmetrical opened-conical forms joined at their narrower ends. Although only one complete vessel was recovered, there are at least three other supports in the entire ceramic assemblage at the site.

F6. Urns with prominent necks. There are two ceramic vessels characterised by the development in height of their necks.

F7. This consists of a single vessel with a carinated profile and a closed structure which distinguishes it from the F1 vessels.

The last four types only represent 4% of the total pottery from the site.

The ceramic assemblage of Genó also contains vessels with variable sizes (Maya *et al.* 1998). A division based on the *size index* (maximum diameter * height / arithmetic mean of the set of values) (López-Cachero 2005: 186) has been established with the aim of grouping the vessels according to their proportions (Annex Tab. 3). Three groups of vessels have been established: small size (vessels up to 2 l), medium size (capacity ranging from 2 to 16 l) and large size (from 18 to more than 60 l).

RESULTS (I): ANALYSIS OF MACRO-TRACES AND RECONSTRUCTION OF POT-FORMING PROCESSES

This section presents a detailed description of each forming sequence and the photographs of macro-traces (Annex Figs. 1 to 7).

Ceramic macro-traces were photographically recorded using a digital camera alternating two lenses (an intermediate lens 18-55 mm and a macro lens 90 mm). The photography was carried out by controlling the entry of natural and artificial light into the room, with a static support and auxiliary LED lights. The scale of the photographs corresponds to the original scale of the traces. The description of traces is based on two methods that allow us to systematically describe macro-traces and the internal structure of vessels in the radial plane (Livingstone Smith 2007; García Rosselló and Calvo Trias 2013; Cámara 2019).

1. Forming process with thin or partially deformed coils (GA1)

The first forming method comprises a series of 74 vessels with similar macro-traces that preserve the profile from the base to the rim or from the belly-shoulder to the rim. Three additional profiles which preserve the lower part of the belly and the base but cannot be individualised also present a similar morphology of traces associated with this forming method.

---

[1] López-Cachero, F. J. 1998: *Estudio de la habitación 2 de Genó: una aproximación al conocimiento del espacio doméstico de las comunidades de CC.UU Antiguos en el Bajo Segre*. Unpublished dissertation. Universidad de Barcelona. Barcelona.

[2] Size indexes, with others referring to the vessel's profile, were previously defined by Picazo (1993) and were applied by one of the authors in the study of the ceramic assemblage of house H-2 of Genó (López-Cachero 1998) and later to the whole ceramic assemblage of the site (Maya *et al.* 1998).

The bases present staggered and circular fractures at the bottom and the beginning of the belly (Annex Fig. 1c). In the radial plane, the cross-sections are characterised by a heterogeneous internal structure with subcircular configurations (Annex Fig. 1d). The combination of these traces suggests that the bases were formed using a spiral coil with discontinuous digital pressures (García Rossello and Calvo Trias 2019). In some cases, an additional coil was added on the external edge of the bases. This forming technique is also identified in nine additional non-individualised bases, with a lateral added coil or an additional coil added below the base and forming a foot.

From the belly to the rim the vessels present a series of staggered vertical fractures and horizontal linear fractures (Annex Fig. 1b1). The topography of the surfaces shows wavy burrs and horizontal variations (Annex Fig. 1b1). These macro-traces evoke the use of the coiling technique for forming the belly and the rim. Small-sized vessels usually have a continuous single fracture in the lower part of the carinated profile, suggesting that they were built in at least two drying phases. In contrast, the development of several continuous linear fractures on the medium-large sized vessels (Annex Fig. 1c) indicates that multiple drying phases were used in order to avoid the collapse of the containers (Manem 2008: 32).

In the radial plane, the cross-sections of the belly are characterised by a heterogeneous structure, with a regular distribution of pores and particles forming 'C/S/Z'-shaped configurations (Annex Fig. 1a2-b2). These configurations may correspond to thin superimposed coils which are then deformed by thinning operations (Livingstone Smith 2007: 121-122) or coils with an oblique alternate overlapping (Martineau 2000: 157-158). The observed configurations on the vessels analysed can be associated with partially or non-deformed coils that are slightly internally and externally overlapped. The rim is formed with a last coil with an internal overlapping, external overlapping or superimposed.

The surfaces of several vessels were modified by scraping, with U-shaped grooves (Annex Fig. 1b1), leading in some cases to trimming, forming erratic striations and deeper grooves (Roux 2019: 177) (Annex Fig. 1a1). In some vessels, the use of discontinuous digital pressures is also observed (irregular topography with hemispherical depressions) and an external layer of clay is added on a single jar by means of digital pressures and stretching out the clay.

2. Coiling and then shaping with the beating technique (GA2 & GA8)

The second forming method is identified in 53 vessels formed by the coiling technique, to which the beating technique is then applied to shape the upper and lower parts of the belly (GA2). Furthermore, the measurement of coils in the cross-sections enabled us to detect up to four additional vessels with thicker coils than the previous ones, which were also shaped with the beating technique (GA8) (see Annex Results (II)).

Several macro-traces can be detected on the base, the belly and the rim associated with the coiling technique: wavy horizontal variations in the inner surface, staggered vertical fractures, horizontal lineal fractures and subcircular/oblique configurations in the radial plane (Annex Fig. 2a2-b2).

The external surfaces show a series of traces produced as a result of applying percussion on the belly and shoulder. The external topography shows sub-circular flat areas (Annex Fig. 2a1-b1) with a compact microtopography and inserted grains (Annex Fig. 2a3). The cross-sections show a foliated aspect, with a vertical orientation of pores and particles associated with oblique and subcircular configurations of deformed coils (Annex Fig. 2a2-b2). Altogether, these macro-traces indicate the use of the beating technique once the vessels were built with the coiling technique.

Percussion can be carried out with tools of different nature and morphology (stone, ceramic hammers or wooden paddles), with or without an anvil (Mayor 2010; Lara 2017: 98). In some vessels, the observation of hemispherical depressions or concavities on the inside may indicate that some kind of tool or the hand was used as an anvil (Manem 2008: 42). Moreover, several vessels preserve grooves on the internal surfaces, which suggest that the inner surfaces were also modified or were scraped.

3. Moulding over a convex support and hammering (GA3)

The GA3 method has been reconstructed based on several vessels (n = 5) in which the base and the lower belly were formed by moulding over a convex support and hammering the outer surface. In turn, the upper belly and the rim were formed with the coiling technique.

The profile and the inner surfaces of the base and the belly are regular, without irregularities and presenting vertical fractures (Annex Fig. 3a2-a3). In several vessels some laminar fractures can also be detected on the inner surface. In contrast, the topography of the outer surface has several flat areas (Annex Fig. 3b1). In the radial plane, the

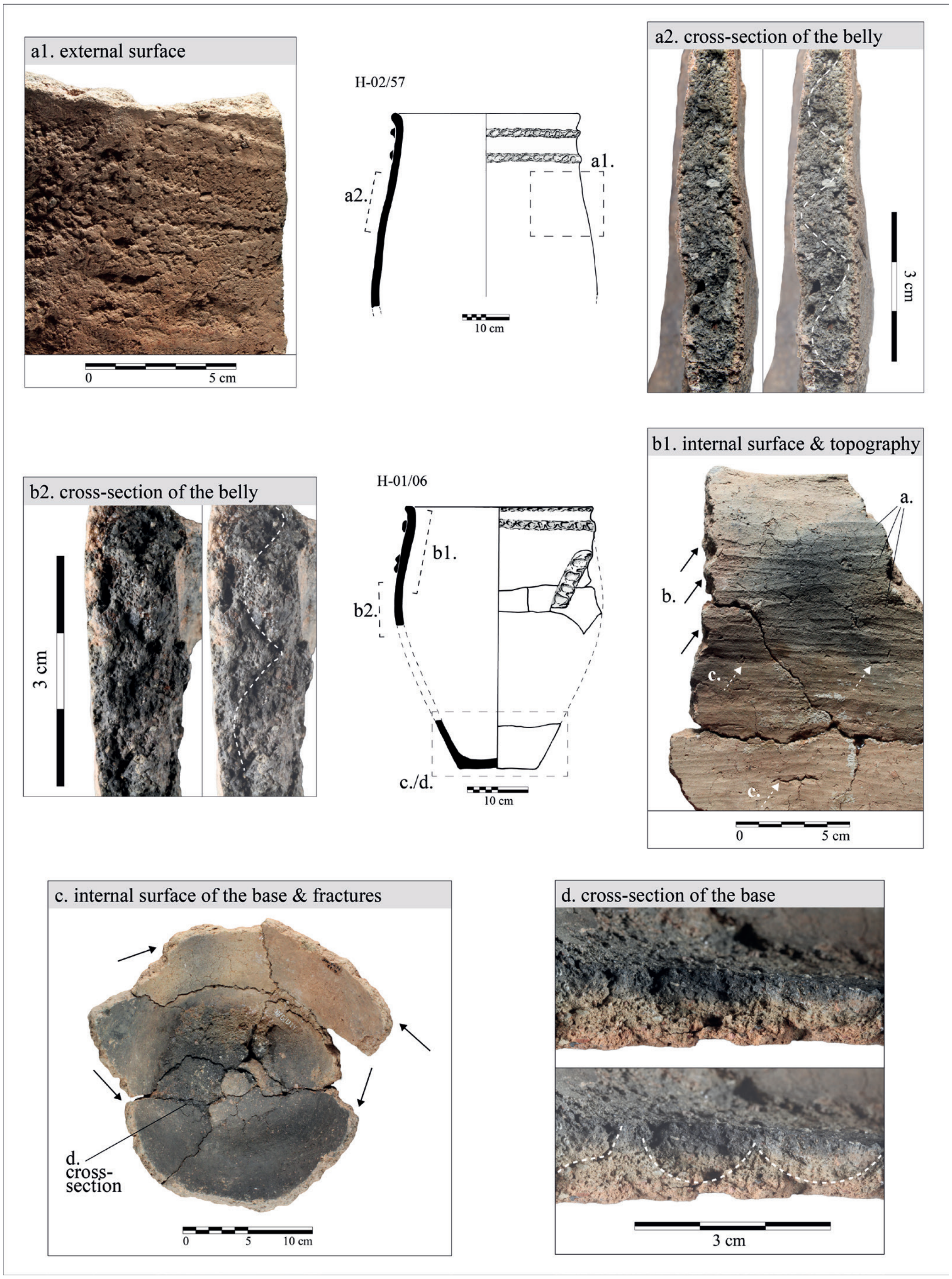

Annex Fig. 1. Macro-traces associated with the GA1 forming method. a1. Erratic striations and horizontal grooves with marked edges and flat sections on the external surface of the belly. a2-b2. Cross-section of the belly with S/Z-shaped configurations. The orientation of particles and voids is subcircular to oblique. b1. Horizontal grooves with marked edges and U-shaped sections (a), staggered vertical fractures (b) and horizontal wavy variations and fissures (c). c. Continuous horizontal fractures on the lower part of the belly (black arrows) and staggered fractures on the base (d). d. Sub-circular configurations in the cross-section of the base. The porosity and a-plastic particles are regularly distributed forming sub-circular units. Altogether, these macro-traces indicate that the bases were formed with a spiralled coil with discontinuous pressures, while the vessel's belly was formed with coils (partially or not deformed) that were slightly internally-externally overlapped. Surfaces were scraped (a2) or trimmed (a1) to modify the topography of the surfaces during or after the forming.

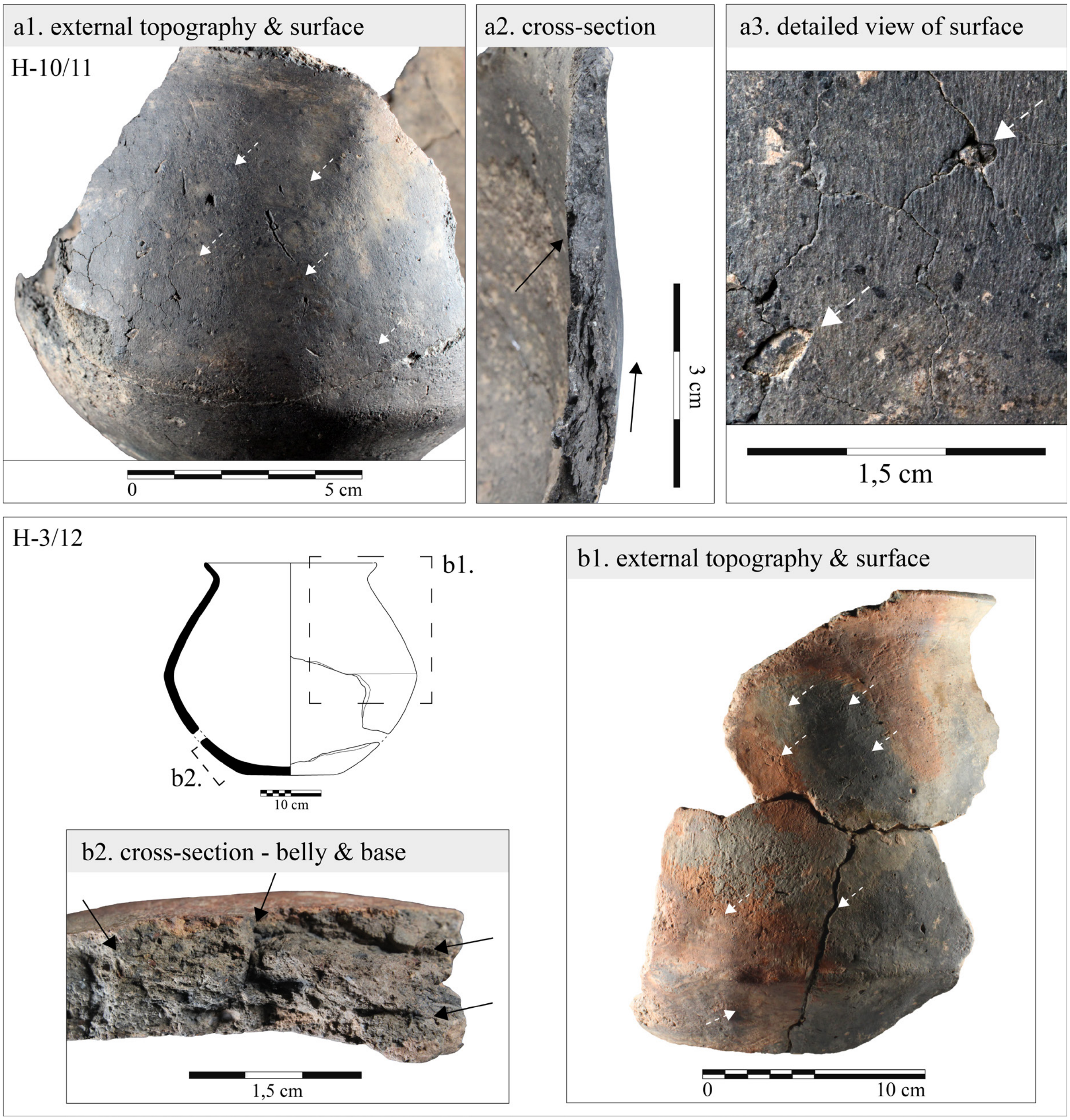

Annex Fig. 2. Macro-traces associated with the GA2 forming method. a1-b1. Circular and sub-circular flat areas located on the external surface of the shoulder and the belly. Flat areas are randomly distributed and overlap each other. a2-b2. Vertical configuration (foliated aspect) with oblique/subcircular deformed configurations in the cross-sections. The orientation of particles and voids is vertical, although some oblique configurations associated with coils can be observed. a3. External surface with inserted grains and compact microtopography. These traces indicate that the vessels were formed with the coiling technique (oblique/subcircular deformed configurations) and then were shaped with the beating technique.

internal structure is compressed and has a foliated aspect (Annex Fig. 3b2). Altogether, these macro-traces indicate that the lower parts of the vessels were moulded on a support and hammered, leaving flat areas (García Rosselló and Calvo Trias 2013: 173) and compressing the internal structure (Livingstone Smith 2007: 122). Once the lower part was placed upside down, the shoulder and the rim were built with the coiling technique, showing a similar morphology of traces to the previous methods: staggered vertical fractures, horizontal wavy variations on the surfaces and hemispherical and elongated depressions.

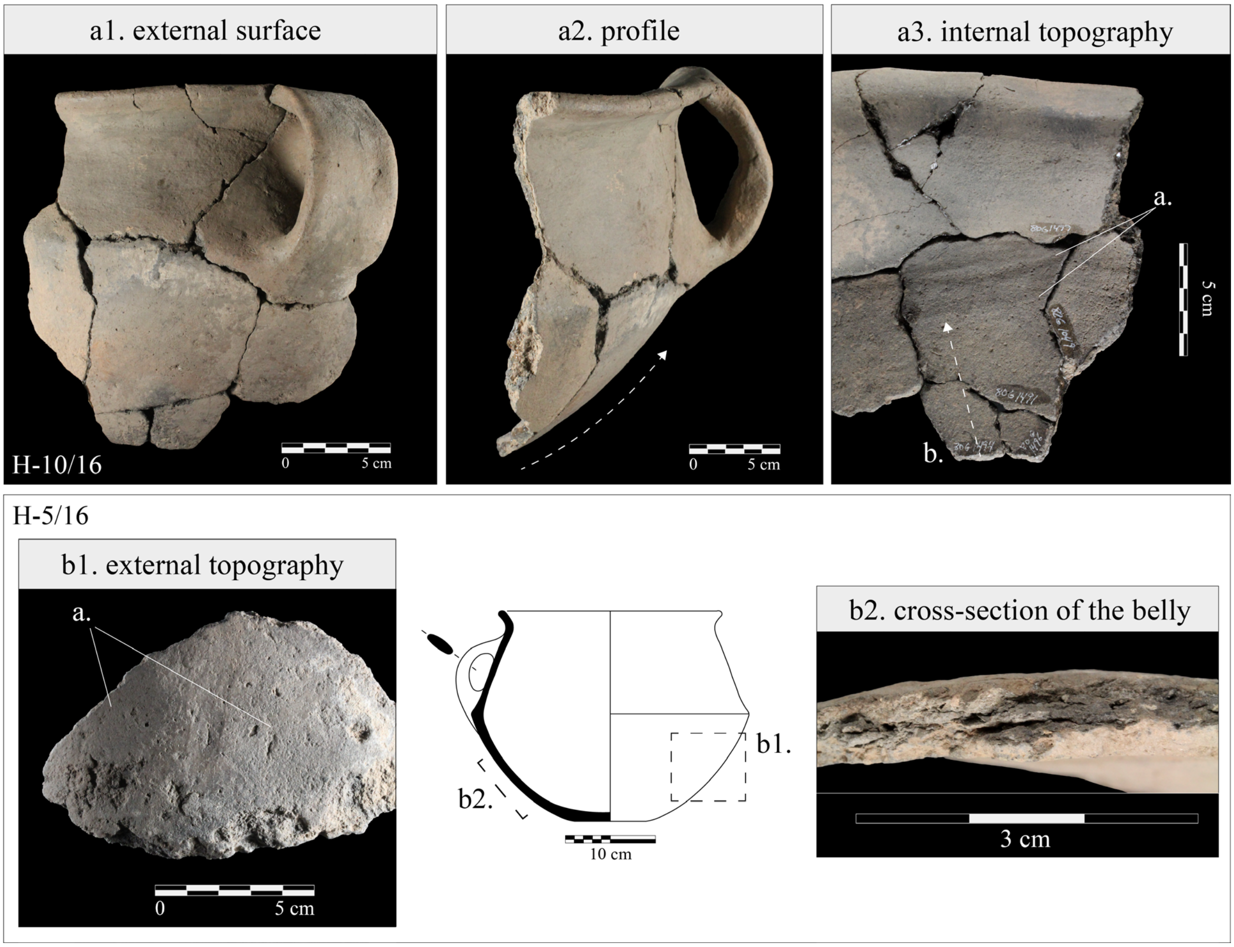

Annex Fig. 3. Macro-traces associated with the GA3 forming method. a1-a2. Regular profile of the lower part of the belly. a3. Regular internal topography of the belly (a) with horizontal variations at the beginning of the inflexion and the shoulder (b). b1. Flat areas on the external surface of the belly (a). b2. Vertical configurations in the cross-sections of the belly parallel to the surfaces (foliated aspect). The combination of these traces suggest that the base and the belly were formed by moulding and hammering over a convex support whilst the upper part was built with the coiling technique.

4. Forming process with coils shaped by pressure against a concave support (GA4)

This forming method is recognised in a series of 11 vessels with diagnostic traces that suggest the use of an external support to shape by compression the lower part of vessels previously formed with the coiling technique.

The morphology of traces indicates the initial forming with the use of the coiling technique: the inner surfaces preserve wavy horizontal variations (Annex Fig. 4a3) and the cross-sections are characterised by slightly deformed S-shaped configurations, in some cases indicating that coils were compressed (Annex Fig. 4b2). The internal topography also preserves several hemispherical depressions (Annex Fig. 4b3), which suggests the use of discontinuous digital pressures from the inside. On the outer surfaces a single horizontal wavy depression (Annex Fig. 4b1) or a ridge (Annex Fig. 4a2) can be observed below the carinated profile. The correlation of these traces indicates that the lower parts of the vessels were coiled and then shaped by compression against a concave support. The upper part of the belly and the rim were also formed with the coiling technique before or after removing the external support. Once the support was removed, several vessels (n = 8) were also beaten due to the presence of circular flat areas on the external surface of the belly.

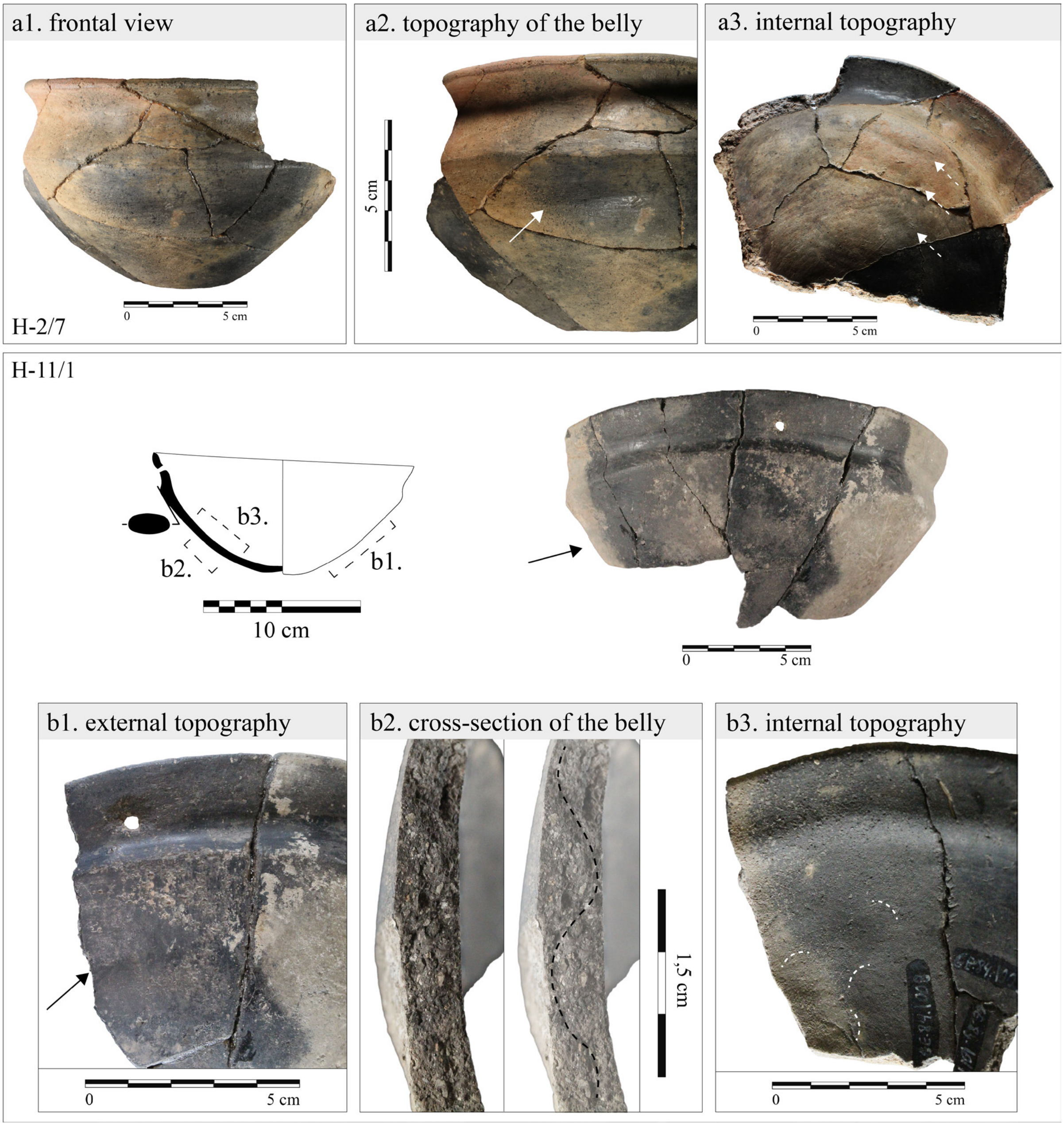

Annex Fig. 4. Macro-traces associated with the GA4 forming method. a-b. Horizontal individual ridge (a2) or wavy variations (b1) located at the external surface of the belly below the inflexion. a3. Horizontal variations and fractures on the internal topography of the belly. b2. S-shaped configurations in the cross-section of the base and the belly. Particles and voids appear partly compressed with a vertical orientation parallel to the surfaces. b3. Hemispherical depressions caused by digital pressures on the internal topography of the belly under the inflexion of the profile. The combination of these traces suggest that vessels were formed by coiling and were then shaped by compression against a concave support. The upper part and the rim were also built with coils when the support was still kept or after its extraction.

5. Forming process with very thick superimposed coils (GA5)

The GA5 forming method comprises a series of seven vessels with the base formed by thick coils in a spiral and the belly and rim built with very thick superimposed coils that can be slightly overlapped from the inner and the outer surface.

The morphology of traces preserved in the topography of the surfaces as well as the fracturing patterns evoke the use of coils: annular fractures at the bases, staggered vertical fractures on the bellies and wavy horizontal variations and burrs on the inner and the outer surfaces (Annex Fig. 5b). In turn, the cross-sections show O-shaped configurations (Annex Fig. 5a1) that may be overlapped in the lower parts of the belly of the largest vessels, doubling the thickness of the walls (Annex Fig. 5a2). Configurations and measurements in the transversal fractures suggest the use of very thick superimposed coils, especially when compared to the coils used in the other forming methods (see Annex Results (II)). This system of thick overlapped coils towards the inner and the outer sides leads to a thickening of the walls and increases the weight of the vessels (Calvo Trias and García Rosselló 2012; Calvo *et al.* 2016).

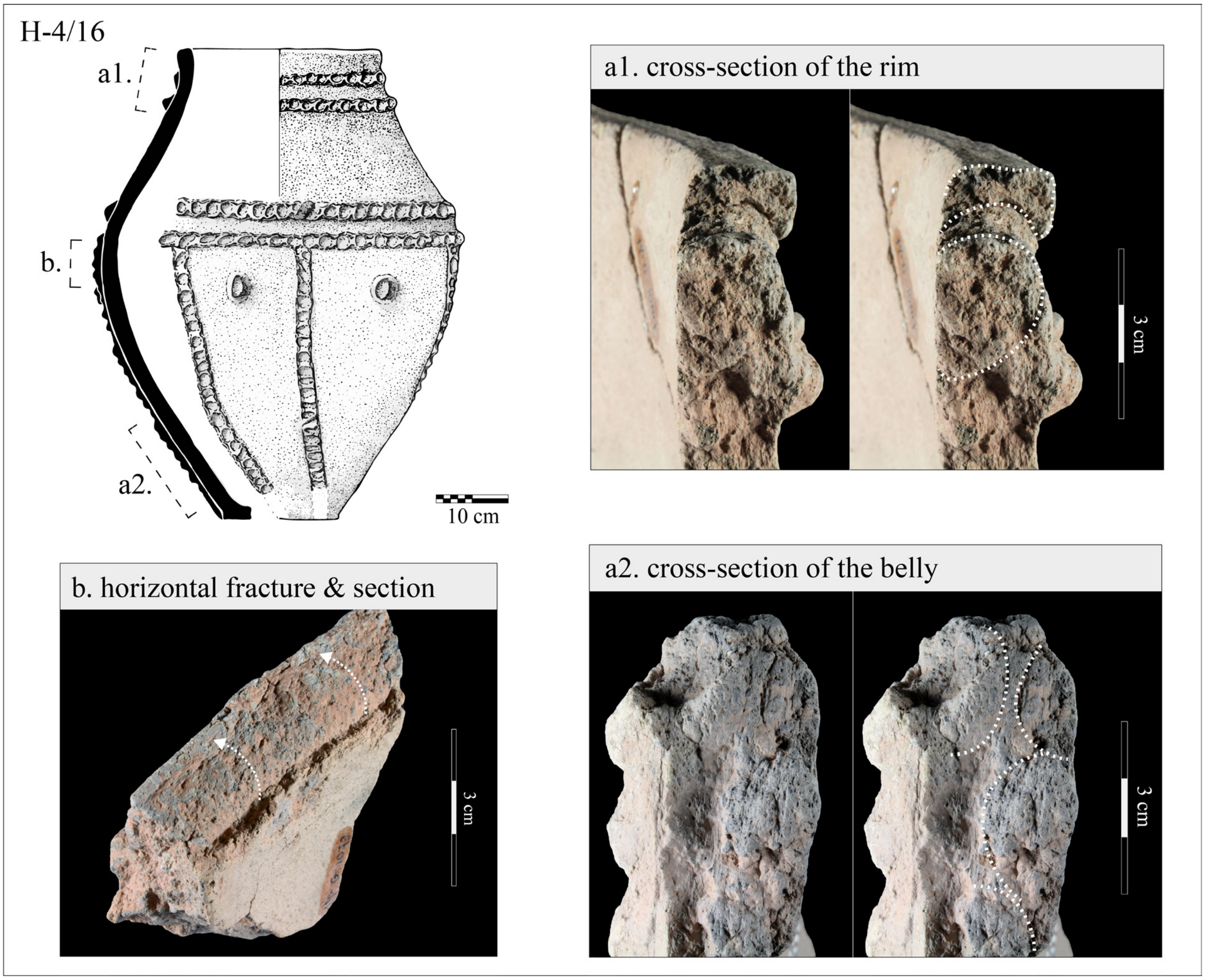

Annex Fig. 5. Macro-traces associated with the GA5 forming method. a1. Circular configurations (O-shaped configurations) in the cross-section of the rim, which suggest the use of thick superimposed coils. a2. Circular configurations in the cross-section of the lower part of the belly, which indicate that coils were also superimposed and placed from the inside and the outside. b. Horizontal fracture of the belly with an inverted U-shaped section towards the outer wall. The development of continuous linear fractures indicates that not only were the vessels constructed following several drying phases, but also that coils were slightly internally and externally overlapped.

6. Forming process with slabs or very elongated elements (GA6)

This forming method has been recognised in a number of 15 vessels which were formed by several assembled elements at the base (possibly spiral coils) and very elongated elements or juxtaposed slabs at the belly. Two non-individualised profiles which preserve the base and part of the belly also have a similar morphology of traces associated with this forming method.

The bases show staggered and annular fractures that indicate the use of assembled elements (Annex Fig. 6b3), possibly the assembly of large coils in a spiral or even slabs. It is just at the edge of the bases where a vertical slab is placed and the construction of the belly begins.

Along the belly, the inner (Annex Fig. 6b3) and outer (Annex Fig. 6b1-b2) surfaces exhibit wavy horizontal variations, spaced among them, which coincides with the development of long staggered vertical fractures. Moreover, several vertical fissures and burrs can be observed, which divide the horizontal variations in each row (Annex Fig. 6b3). In the radial plane, the cross-sections present long vertical and oblique configurations, suggesting the use of very elongated elements. Altogether, this morphology of traces forming segmented elements in the same row can be associated with the use of juxtaposed slabs or very elongated elements to build the belly of the vessels (Rye 1981: 80; Vandiver 1987; Roux 2019: 166-168).

In several vessels, the shape of these elements corresponds to elongated rectangular elements (Annex Fig. 6b3) that can be superimposed or internally overlapped over each other (Thér *et al.* 2019). After being assembled, these elements were also modified by using discontinuous digital pressures (diagonal and elongated digital depressions on the external topography) (Annex Fig. 6b2). The rim is then finished with one or two coils: internally overlapped, externally overlapped or superimposed.

7. Forming process with horizontal slabs, shaped with the beating technique (GA7)

This forming method was recognised in two vessels that were built with large assembled elements or slabs, which were shaped with the beating technique afterwards.

In these two vessels the forming technique of the base cannot be inferred since in both cases they are intact or restored. The belly has a similar morphology of traces to the previous forming method: long and regular horizontal and vertical fractures (i) (Annex Fig. 6a2) and wavy and spaced horizontal variations in the inner surface (ii). The outer topography of the belly shows, in contrast, a series of randomly distributed flat areas and overlapping concavities (Annex Fig. 6a3). The correlation of these traces suggests that the vessels were constructed by successive juxtaposed slabs in horizontal rows, which were beaten after their construction. The rim is formed with one or two assembled coils with external overlapping.

8. Insertion systems of grip and secondary elements

The analysis of grip elements also provides data on their manufacturing process and the insertion systems on the walls (Tab. 2). The ceramic productions of Genó are characterised by the use of oval-section handles with or without a cylindrical button appendix. The appendix buttons and the handles present a protuberance at their edges, which is associated with a complete insertion by drilling the walls or drilling the upper part of the handles (Annex Fig. 7). The use of complete insertions is detected in a total of five individual handles and 11 vessels produced with different methods: GA1 to GA4 and GA6. This is the most common attachment system of handles, although it cannot be identified in all vessels since the handles are not generally detached from the walls.

The other secondary or plastic added elements correspond to lugs or, more frequently, digitally impressed cordons, the former inserted by means of a concavity in the walls and the latter generally joined by applying pressure directly to the surfaces. Cordons are widely used on vessels produced with GA1 to GA7. Conversely, circular lugs are less-frequent and their attachment system was detected in a couple of jars produced with GA1 and GA5. Small vessels also contain small lugs, which were drilled twice before or after being added to the vessels.

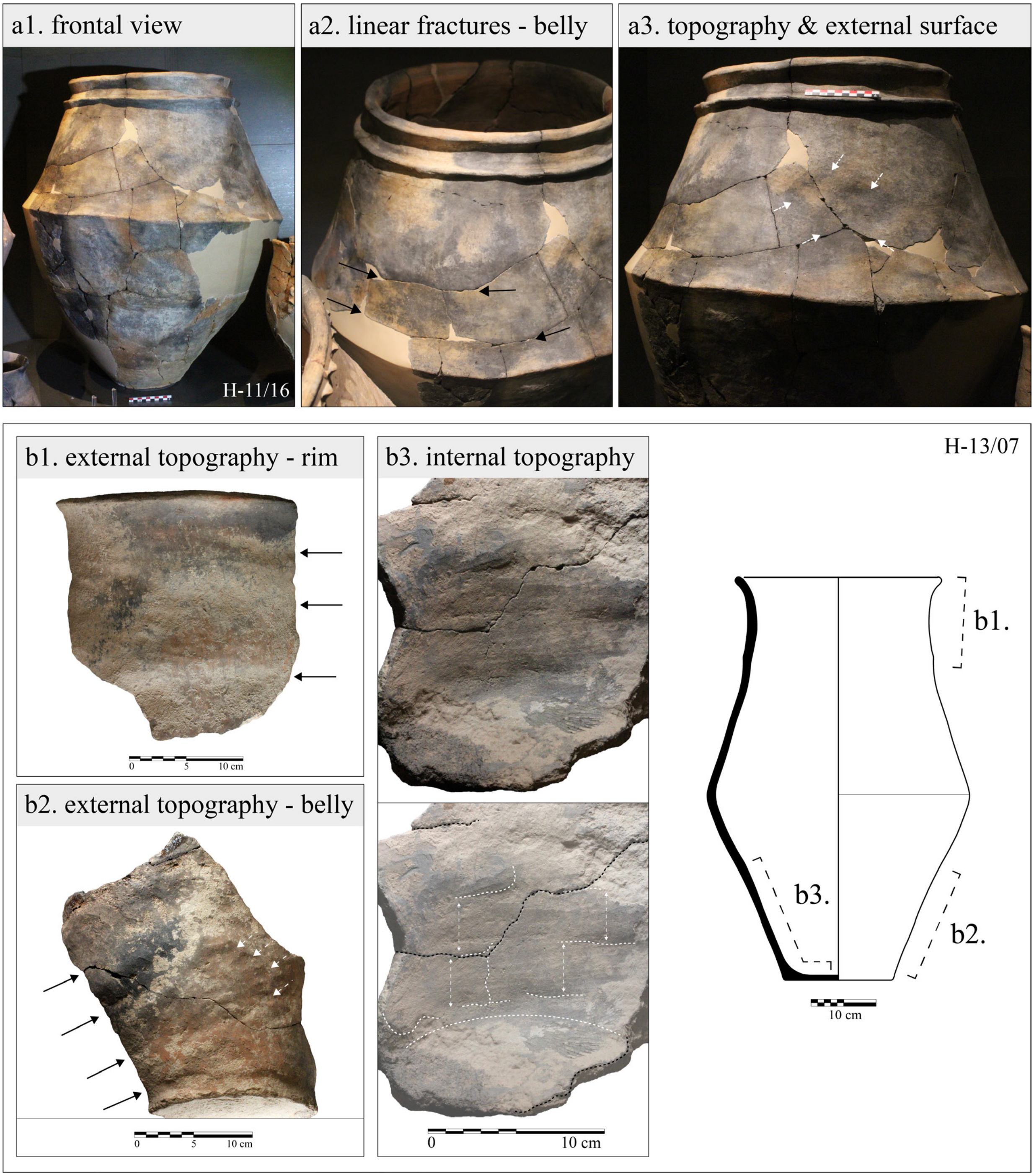

Annex Fig. 6. Macro-traces associated with the GA6 and GA7 forming methods. a1-a2. Horizontal and vertical regular fractures observed on the internal and external surfaces of the belly and shoulder. b1-b2. Long horizontal wavy variations on the external topography of the upper and lower parts of the belly (black arrows). Horizontal variations appear spaced among them with hemispherical depressions (white arrows, b2). b3. Long staggered vertical fractures (black dashes) and long horizontal variations (white dashes) on the internal topography of the belly. Horizontal fractures and wavy variations merge together into long horizontal elements (white vertical arrows), which are divided in each row by vertical fissures and burrs (white dashes). Altogether, these traces suggest the forming process with slabs or very elongated elements. In the GA6 method, slabs are modified with discontinuous pressures (digital elongated depressions on the surface, 6b2), whilst in the GA7 method slabs are shaped with the beating technique after their construction (flattened areas and concavities on the external topography, 6a3).

Annex Fig. 7. Macro-traces associated with the insertion system of button appendix handles. Cylindrical protuberance located at the edge of the button appendix handle, inserted on the top of an oval-section handle.

RESULTS (II): QUANTITATIVE ANALYSIS OF THE HEIGHT AND THICKNESS OF THE ASSEMBLED ELEMENTS

Annex Tabs. 4 and 6 include the descriptive statistical parameters of the measurements (height and thickness) of the assembled elements used in six of the seven forming sequences (GA1 to GA6), which were divided according to the proportions of the vessels (Fig. 3 and Annex Fig. 8). Annex Tabs. 5 and 7 present the results of the Levene's test, used to evaluate the equality of variances, and the Welch's test (ANOVA), used when variances were unequal, both with a probability threshold of $\alpha = 0.05$ (Hammer *et al.* 2001).

– The GA1 method shows intra-group variability, with partially or non-deformed coils, which increase in both height and thickness according to the vessel's size. Overall, the height of the coils from the belly ranges from 6.1 (for a thickness of 4 mm) to 28.5 mm (for a thickness of 17.9 mm), detected by measuring the configurations in the cross-sections.

– The GA2 method also presents intra-group variability in the coil's height and thickness, with values similar to GA1. The coils measurements associated with GA2 vary between 6 mm and 23.8 mm for a thickness of 4 and 11

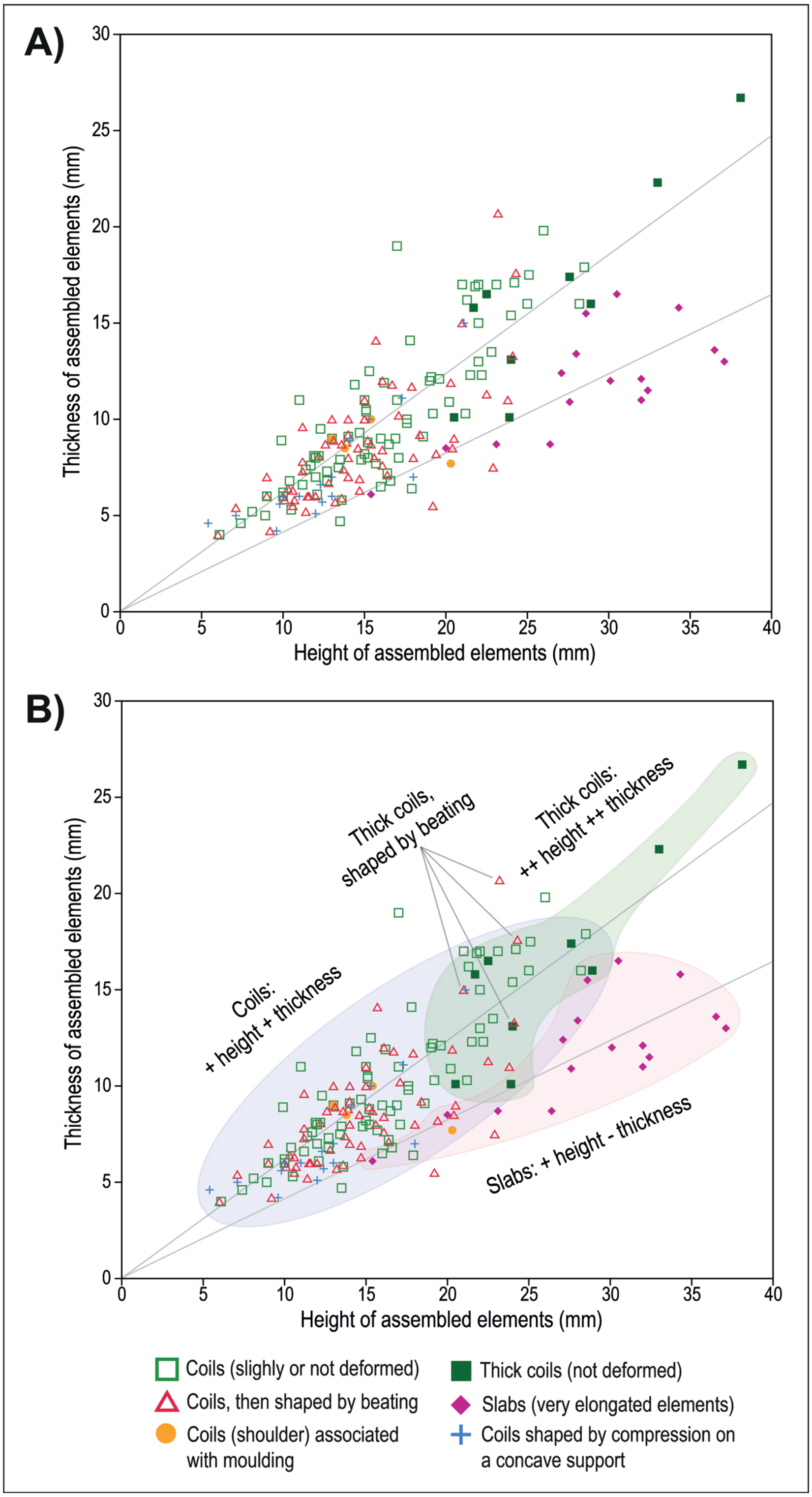

Annex Fig. 8. Scatterplot with the height and thickness (wall-thickness) of the assembled elements measured from the upper and lower parts of the belly of the ceramic vessels of Genó. A. Regression lines. B. Outlines with the distribution patterns of values.

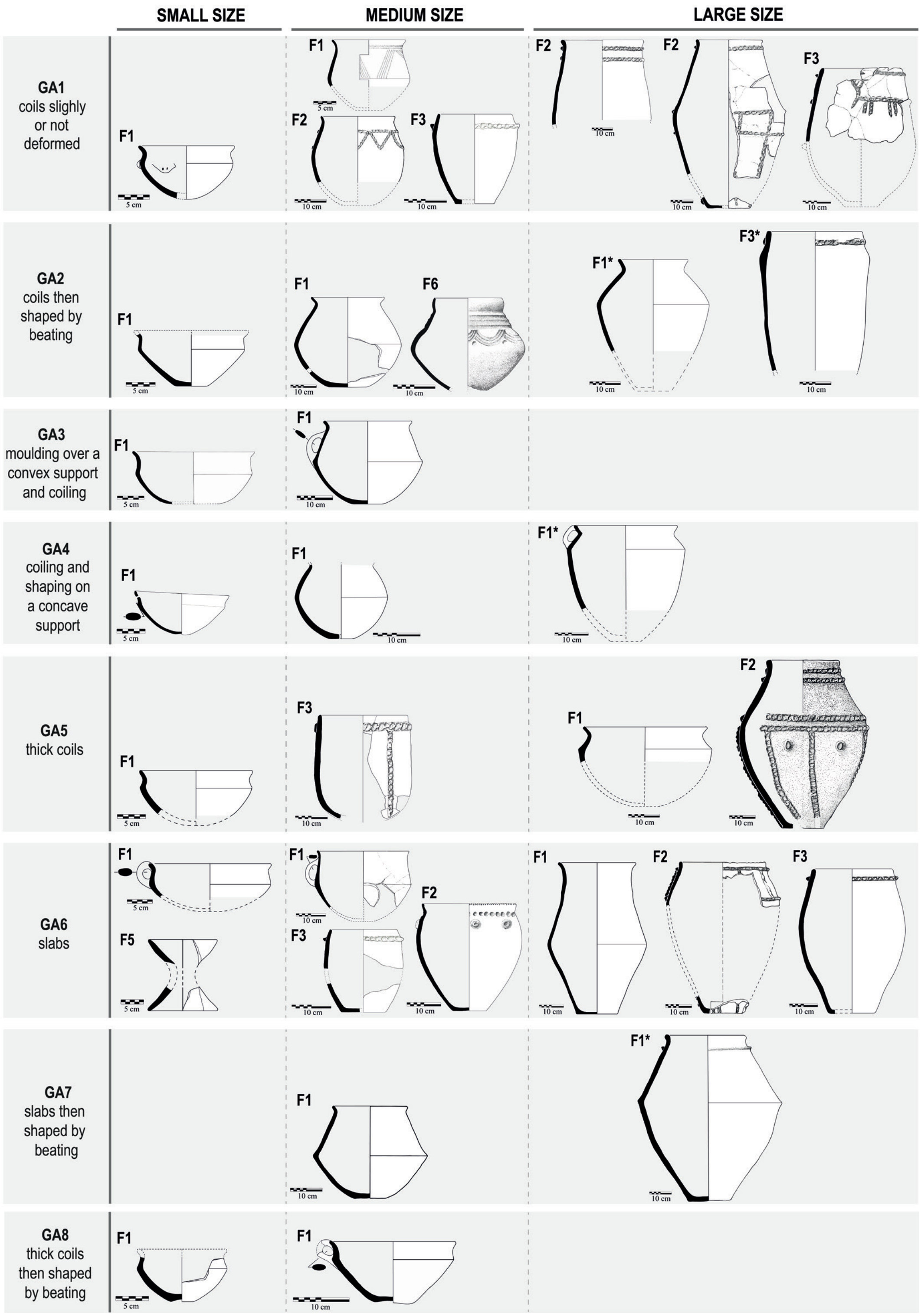

Annex Fig. 9. Examples of vessels' shapes and sizes attributed to each of the eight forming methods (GA1-GA8). The numeric code (F1 to F6) refers to the type of vessels: F1 = carinated profiles; F2 = S-shaped opened profiles; F3 = closed profiles; F5 = biconical supports; F6 = profiles with neck. F1*-F3* correspond to the only large-sized vessels associated with the methods GA2, GA4 and GA7.

mm respectively. Several small-medium sized vessels stand out with coil measurements similar to the GA5 method (GA2 outliers), indicating that some vessels were also produced with thick coils and were then shaped with the beating technique. In these cases, with thicker coils (detected in 4 vessels), the coil height ranges from 14 to 24.4 mm for a thickness of between 10 mm and 17.6 mm. Therefore, these vessels can be considered as part of another forming sequence (GA8), distinguished from the rest by the use of thick coils, but also from GA5 by the use of the beating technique.

– The measurements of coils used in the GA3 (upper belly) and GA4 methods are analogous to the previous forming methods. The coil height in the upper belly of GA3 ranges from 13 mm, for a thickness of 9 mm, to 20.3 mm, for a thickness of 7.7 mm. The coil height of the belly of GA4 oscillates between 5.4 mm (for a thickness of 4.6 mm) and 21.1 mm (for a thickness of 15 mm). Nonetheless, more lengthened coils compared to a lower thickness of the walls can be seen in those vessels compressed against a concave support (GA4).

– Vessels produced with the GA5 method have higher and thicker coils than the previous ones. By measuring the coils in the cross-sections, the coil height in the belly ranges from 18.3 to 38.1 mm for a wall-thickness of between 12.5 mm and 26.7 mm. However, some large vessels of GA1 and GA2 are quantitatively similar to the lowest measurements of vessels produced with the GA5 method (see Fig. 3). These data indicate that, except for a few exceptions (*e. g.,* Annex Fig. 5), the three forming methods (GA1, GA2 and GA5) cannot be completely differentiated at a quantitative level in some cases. It should also be noted that several small-medium sized vessels assigned to the GA8 method (GA2 outliers) have similar height and coil thickness to this method, although they differ from GA5 in the shaping process with the beating technique.

– Vessels built with slabs or very elongated elements (GA6) are higher and more elongated compared to the coils of GA1 to GA4, but have a similar thickness to these forming methods. These elements were measured in the cross-sections or by taking into account the spaced horizontal variations on the surfaces. In the lower belly, the height measurements vary from 23.1 mm (for a wall-thickness of 8.7 mm) to 37.1 mm (for a wall-thickness of 13 mm). In the upper belly, the dimensions vary between 15.4 mm (thickness of 6.1 mm) and 34.3 mm (thickness of 15.8 mm). Within this method the lowest height values, related to small or medium vessels, also coincide with those of methods GA1 and GA2. The two remaining vessels from GA7, also associated with the use of slabs or large assembled elements, were not measurable since they have been partially or completely restored.

Excluding some outliers for both height (GA2) and thickness of coils (GA2 & GA4) (Fig. 3), the results of the Levene's test and the unequal-variance test (Welch's ANOVA) confirm that significant differences existed between the means of the height and thickness of the assembled elements analysed according to their corresponding forming methods (i) as well as among the vessel sizes in the case of GA1 and GA2 methods (ii) (Annex Tabs. 4 to 7).

RESULTS (III): SPATIAL DISTRIBUTION OF POT-FORMING METHODS AT INTRA-SITE SCALE

The spatial distribution of the pot-forming sequences has been analysed by plotting the frequency of techniques for each house in the plan of the settlement (Annex Fig. 10) and using the Correspondence Analysis (CA) (Annex Fig. 11, Annex Tabs. 8 and 9).

The spatial distribution shows that GA1 and GA2 methods are located throughout the settlement, although these pot-building sequences dominate in three of the houses that contain the largest quantity of vessels (houses H-2, H-5 and H-10). Both methods were also documented in houses H-7 and H-16, although the low number of preserved and analysed vessels makes it impossible to assess the representativeness of the forming methods in these houses. Moreover, jars produced with GA1 were found in houses H-1 to H-5 and houses H-9 to H-10, while the two jars produced with GA2 were identified in houses H-1 and H-2. Vessels produced using GA3 and GA4 are less frequent and are unevenly distributed throughout the settlement: GA3 is present in houses H-5, H-10 and H-12, while GA4 can be identified in houses H-2, H-5 and H-11. Conversely, GA5 and GA6 were detected in several houses from the north (H-4 to H-6) and the south (H-10 to H-15) at the centre of the site. First, houses H-4, H-14 and H-15 are characterised by the presence of several vessels and one of their jars produced using GA5. Second, house H-5 as well as houses H-11 to H-13 are characterised by a relative frequency of vessels and jars produced with GA6, although other houses also contain some vessels produced with GA6: H-4, H-6, H-10 and H-14. The method GA7 is only recognised in two vessels from the houses H-3 and H-11, one of which corresponds to a very large jar from H-11. Finally, several vessels associated with GA8 can be found in houses H-2, H-4 and H-13.

The Correspondence Analysis (CA) (Annex Fig. 11) was used to compare the forming methods with the houses (Annex Fig. 10). The first three axes (axes 1/2 and 1/3) reveal significant variability in the distribution (Annex Tab. 9):

– Axis 1 opposes GA5 with the other methods: the group comprised of GA1 to GA4 and the group of GA6 and GA8.

– Axis 2 opposes GA6 with the other methods: the group comprised of GA1 to GA4 and GA5.

– Axis 3 opposes GA8 and slightly GA7 to the other forming methods.

Overall, these results show that, in the distribution of the houses, the two most prevalent forming methods (GA1 and GA2), GA5 and GA6 are distant from each other. In addition, other methods tend to cluster with these prevalent forming sequences: GA3/GA4 with GA1/GA2 and GA6 with GA8 in one of the houses (H-13).

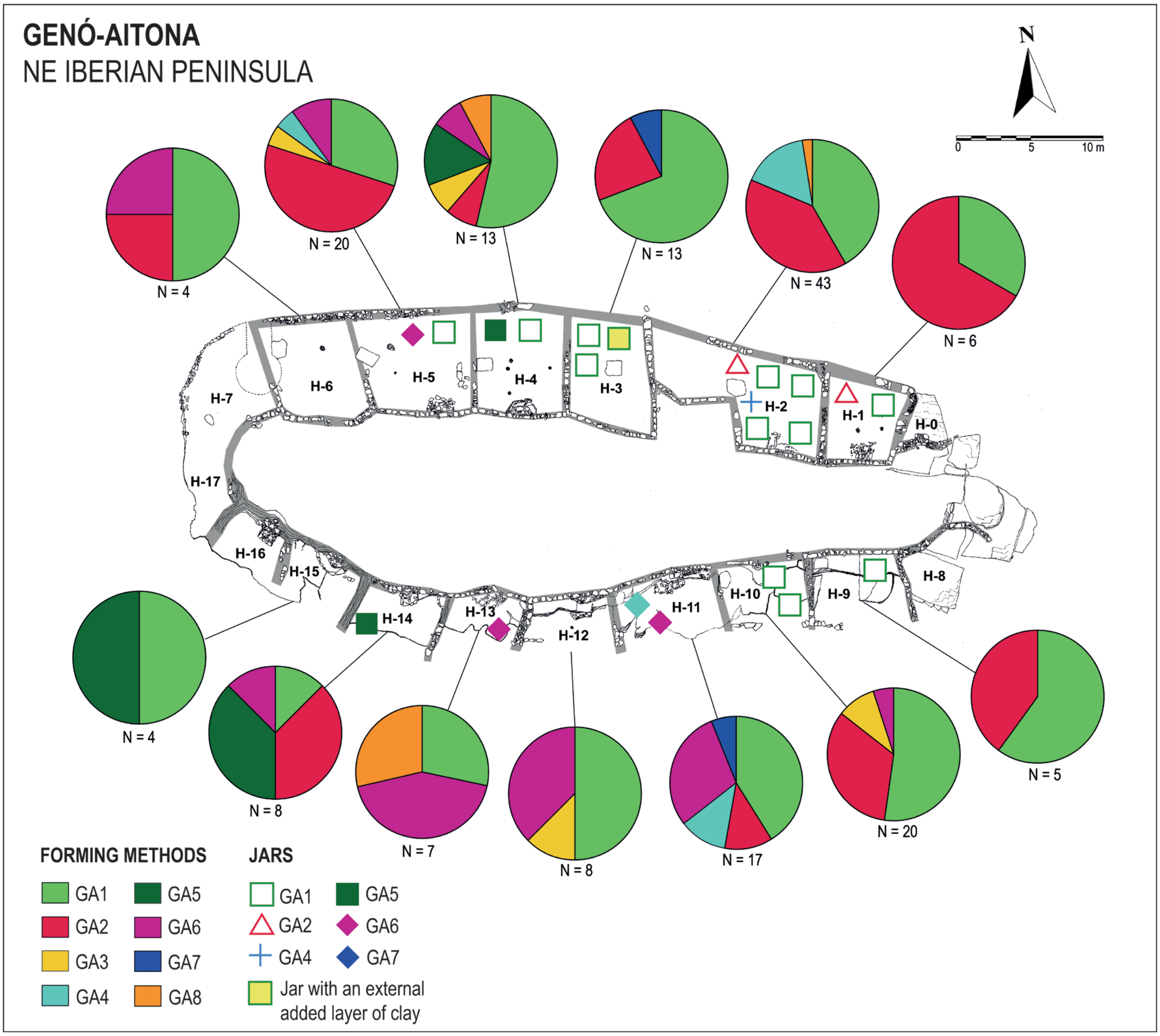

Annex Fig. 10. Spatial distribution of the eight forming methods (GA1-GA8) in each house at Genó-Aitona (GA) and distribution of the large-sized vessels and jars from each house (H-1 to H-14). The distribution includes 171 ceramic vessels and 5 lower-profiles associated with a forming method. Houses H-0, H-8 and H-17 contain a very low number of vessels and data on pottery forming from houses H-7 and H-16 are very limited.

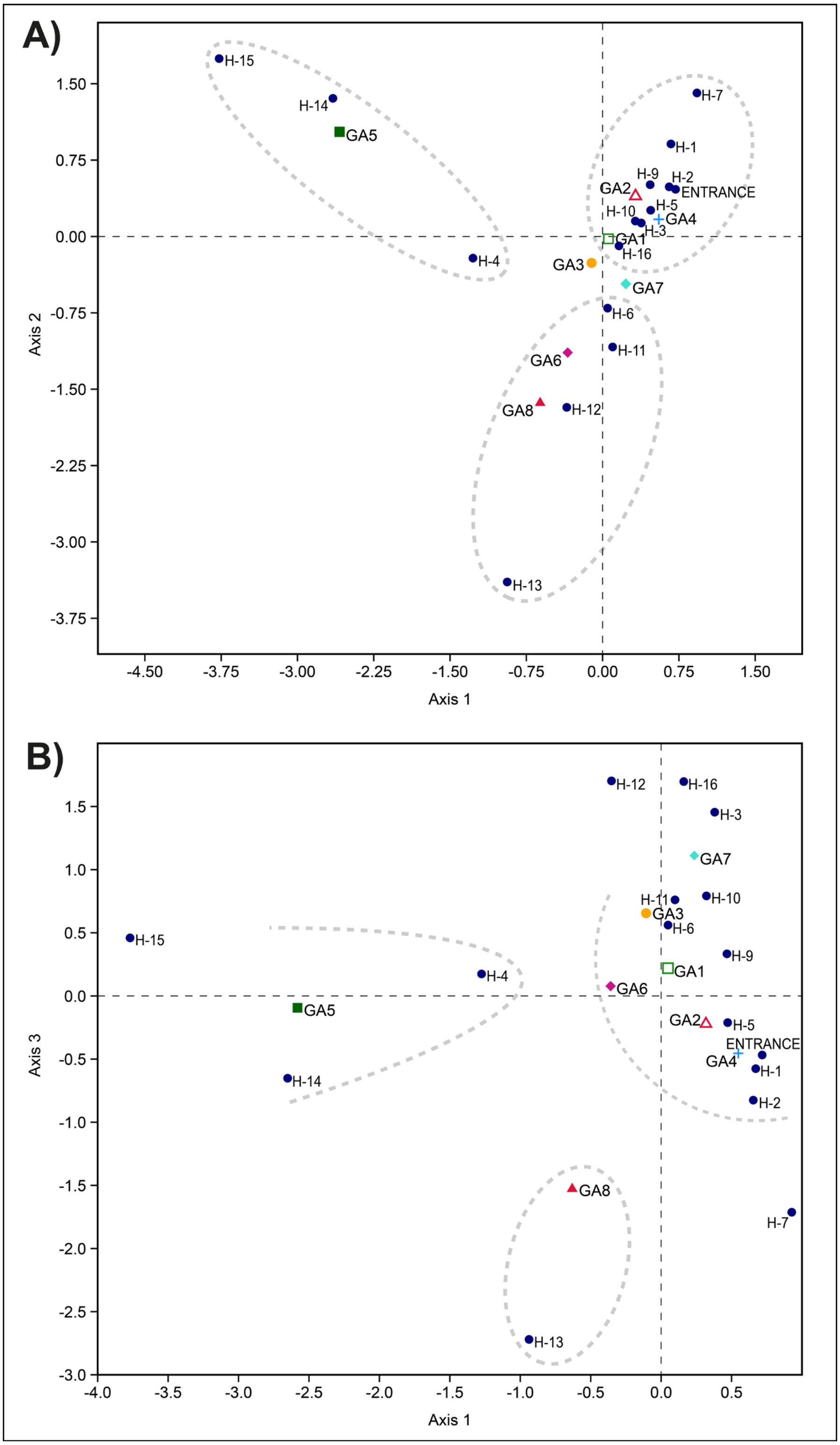

Annex Fig. 11. Correspondence analyses of houses (H-1/H-16) and the eight forming methods (GA1-GA8) at Genó. A. Axes 1 and 2. B. Axes 1 and 3.

Context	Sample	Lab code	BP date	1σ cal BCE (68.3%)	2σ cal BCE (95.4%)	Reference
H-2 Burnt layer	charcoal	GrN-18061	2970±54	1278-1111 (68.3 %)	1383-1341 (6.3 %) 1311-1016 (89.1 %)	Maya *et al*. 1998
H-5 Support beam - roof	charcoal	GrN-18062	2860±90	1192-1177 (3.3 %) 1159-1145 (3.0 %) 1129-915 (62.0 %)	1275-821 (95.4 %)	Maya *et al*. 1998
H-12 Square D-5	charcoal	UBAR-519	2815±45	1042-1036 (2.0 %) 1016-906 (66.2 %)	1112-893 (88.6 %) 879-837 (6.8 %)	Maya *et al*. 1998

Annex Tab. 1. Calibration of radiocarbon dates from Genó with OxCal v.4.4.3 program (Bronk Ramsey 2021) and the IntCal20 atmospheric curve (Reimer *et al*. 2020) in 1 and 2 *sigma* (σ).

Genó Houses	**Number of ceramic elements**					**Estimated number of vessels**	**Number of vessels and bases associated with a forming method**		
	Reconstructed profiles	**Rims**	**Bases**	**Grip ele-ments**	**Total**		**Vessels**	**Bases**	**Total**
Entrance	6	9	0	2	**17**	6	4	0	**4**
H-0	0	0	0	0	**0**	0	0	0	**0**
H-1	6	9	2	2	**19**	7	6	0	**6**
H-2	60	48	7	16	**131**	66	42	1	**43**
H-3	23	15	1	2	**41**	25	13	0	**13**
H-4	16	8	2	0	**26**	19	13	0	**13**
H-5	25	31	5	2	**63**	28	19	2	**21**
H-6	5	2	0	0	**7**	5	4	0	**4**
H-7	5	5	5	0	**15**	6	2	1	**2**
H-8	2	2	0	0	**4**	2	0	0	**0**
H-9	11	3	0	0	**14**	12	5	0	**5**
H-10	27	15	6	3	**51**	30	20	2	**22**
H-11	16	13	3	1	**33**	20	16	3	**19**
H-12	5	12	5	0	**22**	8	6	4	**10**
H-13	7	7	1	4	**19**	7	7	1	**8**
H-14	14	17	0	0	**31**	15	8	0	**8**
H-15	0	7	2	0	**9**	5	4	0	**4**
H-16	4	10	0	2	**16**	4	2	0	**2**
H-17	1	1	0	0	**2**	1	0	0	**0**
SD	9	38	6	4	**57**	9	0	0	**0**
Total	**242**	**252**	**45**	**38**	**577**	**275**	**171**	**14**	**184**

Annex Tab. 2. Number of ceramic elements and vessels from the ceramic assemblage of Genó and number of ceramic vessels analysed in this study. SD = vessels without a referenced location (previous excavations to 1977).

Groups	Size index	Capacity (l)	Types	Total number of vessels
Small size	0.089-0.445	0.15-2	F1, F2, F5	120
Medium size	0.452-0.796	2-16	F1, F2, F3, F6	89
Large size	2.010-9.112	18-110	F1, F2, F3	28

Annex Tab. 3. Categories of vessel's size based on the *size index* (maximum diameter * height / arithmetic mean of the set of values) and their capacity.

	GA1			GA2			GA3	GA4	GA5	GA6
	Small size	**Medium size**	**Large size**	**Small size**	**Medium size**	**Large size**	**Small - medium size**	**Small - large size**	**Small - large size**	**Small - large size**
N. º	29	28	23	24	36	4	4	16	11	16
Min	6.1	9.9	16.2	6	10.6	11.2	13	5.4	18.3	15.4
Max	17.9	22.2	28.5	24.3	24.1	23.2	20.3	21.1	38.1	37.1
Mean	12.41	15.30	21.82	11.54	16.54	17.33	15.63	12.59	25.35	28.82
Variance	9.79	9.90	12.07	13.63	11.98	32.42	10.71	16.14	36.18	33.11
SD	3.13	3.15	3.47	3.69	3.46	5.69	3.27	4.02	6.02	5.75
Median	12	15	22	11.2	15.9	17.45	14.6	12.35	23.9	29.35
Coeff. var	25.21	20.56	15.92	31.99	20.93	32.87	20.94	31.92	23.73	19.97

Annex Tab. 4. Descriptive statistical parameters for the height measurements of the assembled elements used in Fig. 3 and Annex Fig. 8 according to each forming method.

Levene's test for homogeneity of variance, from means	*p* (same):	**0.009659**
Levene's test, from medians	*p* (same):	0.04056
Welch *F* test in the case of unequal variances	*F* =	28.97
	df =	33.1
	p =	**3.368E-13**

Annex Tab. 5. Results of the Levene's and Welch's (ANOVA) tests for the height measurements of the assembled elements. Unequal variance confirmed by Levene's test (for homogeneity of variance, from means) and significant statistical differences (p =) revealed by the unequal-variance Welch's test (ANOVA).

	GA1			**GA2**			**GA3**	**GA4**	**GA5**	**GA6**
	Small size	**Medium size**	**Large size**	**Small size**	**Medium size**	**Large size**	**Small - medium size**	**Small - large size**	**Small - large size**	**Small - large size**
N. º	29	28	23	24	36	4	4	16	11	16
Min	4	6.1	9.8	4	5.2	8.8	7.7	4.2	10.1	6.1
Max	11	12.5	19.8	17.6	14.1	20.7	10	15	26.7	16.5
Mean	6.86	9.40	15.03	7.38	8.72	13.53	8.8	7.12	16.08	11.86
Variance	2.43	3.16	8.00	8.41	5.18	30.46	0.93	8.11	24.68	8.24
SD	1.56	1.78	2.83	2.90	2.28	5.52	0.96	2.85	4.97	2.87
Median	6.8	9.05	16	6.55	8.45	12.3	8.75	6	16	12.05
Coeff. var	22.72	18.92	18.82	39.27	26.09	40.81	10.94	40.00	30.89	24.21

Annex Tab. 6. Descriptive statistical parameters for the thickness measurements of the assembled elements used in Fig. 3 and Annex Fig. 8 according to each forming method.

Levene's test for homogeneity of variance, from means	*p* (same):	**1.313E-05**
Levene's test, from medians	*p* (same):	9.991E-05
Welch *F* test in the case of unequal variances	*F* =	24.46
	df =	34
	p =	**2.349E-12**

Annex Tab. 7. Results of the Levene's and Welch's (ANOVA) tests for the thickness measurements of the assembled elements. Unequal variance confirmed by Levene's test (for homogeneity of variance, from means) and significant statistical differences (p =) revealed by the unequal-variance Welch's test (ANOVA).

Houses	GA1	GA2	GA3	GA4	GA5	GA6	GA7	GA8	Total
H-1	2	4	0	0	0	0	0	0	**6**
H-2	18	17	0	7	0	0	0	1	**43**
H-3	9	3	0	0	0	0	1	0	**13**
H-4	7	1	1	0	2	1	0	1	**13**
H-5	6	10	1	1	0	2	0	0	**20**
H-6	2	1	0	0	0	1	0	0	**4**
H-7	0	2	0	0	0	0	0	0	**2**
H-9	3	2	0	0	0	0	0	0	**5**
H-10	10	7	2	0	0	1	0	0	**20**
H-11	7	2	0	2	0	5	1	0	**17**
H-12	4	0	1	0	0	3	0	0	**8**
H-13	2	0	0	0	0	3	0	2	**7**
H-14	1	3	0	0	3	1	0	0	**8**
H-15	2	0	0	0	2	0	0	0	**4**
H-16	2	0	0	0	0	0	0	0	**2**
Entrance	2	1	0	1	0	0	0	0	**4**
Total	**74**	**55**	**5**	**11**	**7**	**17**	**2**	**4**	**176**

Annex Tab. 8. Contingency table crossing the eight forming sequences (GA1-GA8) with the houses (H-1-H-16).

Axis	Eigenvalue	% of total	Cumulative
1	0.334734	33.435	33.435
2	0.28439	28.407	61.842
3	0.12627	12.613	74.455
4	0.103593	10.347	84.802
5	0.0863883	8.629	93.431
6	0.0528207	5.2761	98.707
7	0.0129427	1.2928	100

Annex Tab. 9. Results of the correspondence analysis from Annex Fig. 11 and Tab. 8. Axes 1 to 3 reveal significant variability on the distribution.

BIBLIOGRAFÍA

Bronk Ramsey, C. 2021. "OxCal 4.4.4 Manual". Available from: https://c14.arch.ox.ac.uk.

Calvo Trias, M. and García Rosselló, J. 2012: "Tradición técnica y contactos: un marco de reflexión centrado en la producción cerámica". In M. Borrell, F. Borrell, J. Bosch, X. Clop and M. Molist (eds.): *Congrés Internacional Xarxes al Neolític - Networks in the Neolithic (Gavà/Bellaterra 2011)*. Rubricatum. Revista del Museu de Gavà 5: 393-401.

Calvo, M.; Albero, D.; García Rosselló, J.; Javaloyas, D.; Gavua, K. and Fornés, J. 2016: "I Like You , I Like Your Pottery : An Ethnoarchaeological Approach to Ceramic Distribution and Acquisition in Northeastern Ghana". *African Archaeological Review* 33: 297-320. https://doi.org/10.1007/s10437-016-9225-z.

Cámara, J. 2019: "Entre trazas, gestos y productores : el análisis traceológico como método de aproximación a las técnicas de modelado en las producciones cerámicas prehistóricas". In X. Clop García, and J. García Rosselló (eds.): *Cerámica prehistórica. Del fragmento a las sociedades humanas, una inverstigación global.* Treballs d'Arqueologia 23: 37-61. https://doi.org/10.5565/rev/tda.94.

García Rosselló, J. and Calvo Trias, M. 2013: *Making Pots. El modelado de la cerámica y su potencial interpretativo*. British Archaeological Reports International Series, 2193. Archaeopress. Oxford.

García Rosselló, J. and Calvo Trias, M. 2019: "Etnoarqueología como experimentación: propuesta para la interpretación de los patrones de fractura". In X. Clop García, and J. García Rosselló (eds.): *Cerámica prehistórica. Del fragmento a las sociedades humanas, una inverstigación global.* Treballs d'Arqueologia 23: 181-202. https://doi.org/10.5565/rev/tda.108.

Hammer, Ø.; Harper, D.; Ryan, P. 2001: "PAST: Paleontological statistics software package for education and data analysis". *Palaeontologia Electronica* 4 (1): 9.

Lara, C. 2017: *Aportes del enfoque tecnológico a la arqueología precolombina: pasado y presente de la alfarería en el valle del río Cuyes y su región (Andes sur-orientales del Ecuador)*. Paris Monographs in American Archaeology, 47. Archaeopress. Oxford.

Livingstone Smith, A. 2007: *Chaîne Opératoire de la poterie. Références ethnographiques, analyses et reconstitution*. Royal Museum for Central Africa (MRAC-KMMA). Tervuren.

López-Cachero, F. J. 2005: *La necrópolis de Can Piteu-Can Roqueta (Sabadell) en el contexto del Bronce Final y Primera Edad del Hierro en el Vallés: Estudio de los materiales cerámicos*. Ph.D. Thesis. Barcelona: Universitat de Barcelona. http://hdl.handle.net/10803/2590.

Manem, S. 2008: *Les fondements technologiques de la Culture des Duffaits (Âge du Bronze Moyen)*. Thesis inédite. Nanterre : Université Paris X-Nanterre.

Martineau, R. 2000: *Poterie, techniques et sociétés. Etudes analytiques et expérimentales à Chalain et Clairvaux (Jura), entre 3200 et 2900 av.J.-C.* Thesis inédite. Dijon: Université de Franche-Comté.

Maya, J. L.; Cuesta, F. and López Cachero, F. J. (eds.) 1998: *Genó: un poblado del Bronce Final en el Bajo Segre (Lleida)*. Publicacions de la Universitat de Barcelona. Barcelona.

Mayor, A. 2010: "Outils de potières au Mali : chaînes opératoires et traditions techniques". *Bulletin de la Société préhistorique française* 107 (4): 643-666. https://doi.org/10.3406/bspf.2010.13971.

Picazo, J. V. 1993: *La Edad del Bronce en el Sur del Sistema Ibérico Turolense, I: Los Materiales Cerámicos*. Monografías Arqueológicas del S.A.E.T., 7. Teruel.

Reimer, P. J.; Austin, W. E. N.; Bard, E.; Bayliss, A.; Blackwell, P. G.; Bronk Ramsey, C.; … Talamo, S. 2020: "The IntCal20 Northern Hemisphere Radiocarbon Age Calibration Curve (0-55 cal kBP)". *Radiocarbon* 62 (4): 725-757. https://doi.org/10.1017/RDC.2020.41.

Roux, V. 2019: *Ceramics and society. A technological approach to archaeological assemblages*. Springer International Publishing. Cham, Switzerland. https://doi.org/10.1007/978-3-030-03973-8.

Rye, O. S. 1981: *Pottery technology: principles and reconstruction*. Taraxacum. Washington, D.C.

Thér, R.; Květina, P. and Neumannová, K. 2019: "Coiling or slab building: Potential of orientation analysis for identification of forming techniques used by Early Neolithic potters". *Journal of Archaeological Science: Reports* 26 (October 2018): 1-14. https://doi.org/10.1016/j.jasrep.2019.101877.